Journal of Assisted Reproduction and Genetics (2020) 37:2159–2170
https://doi.org/10.1007/s10815-020-01859-7

GENETICS

Novel compound heterozygous *DNAAF2* mutations cause primary ciliary dyskinesia in a Han Chinese family

Minghan Sun[1,2] · Yi Zhang[3] · JiyunYang[3] · Yi Wang[2] · Hao Tan[1] · Hailian Wang[2] · Tiantian Lei[2] · Xiaojie Li[2] · Xiaojian Zhang[2] · Wen Xiong[2] · Ke Dou[2] · Yongxin Ma[1]

Received: 8 December 2019 / Accepted: 10 June 2020 / Published online: 7 July 2020

Abstract

Purpose Primary ciliary dyskinesia (PCD), which commonly causes male infertility, is an inherited autosomal recessive disorder. This study aimed to investigate the clinical manifestations and screen mutations associated with the *dynein axonemal assembly factor 2* (*DNAAF2*) gene in a Han Chinese family with PCD.

Methods A three-generation family with PCD was recruited in this study. Eight family members underwent comprehensive medical examinations. Genomic DNA was extracted from the participants' peripheral blood, and targeted next-generation sequencing technology was used to perform the mutation screening. The DNAAF2 expression was analyzed by immunostaining and Western blot.

Results The proband exhibited the typical clinical features of PCD. Spermatozoa from the proband showed complete immotility but relatively high viability. Two novel compound heterozygous mutations in the *DNAAF2* gene, c.C156A [p.Y52X] and c.C26A [p.S9X], were identified. Both nonsense mutations were detected in the proband, whereas the other unaffected family members carried either none or only one of the two mutations. The two nonsense heterozygous mutations were not detected in the 600 ethnically matched normal controls or in the Genome Aggregation Database. The defect of the DNAAF2 and the outer dynein arms and inner dynein arms were notably observed in the spermatozoa from the proband by immunostaining.

Conclusion This study identified two novel compound heterozygous mutations of *DNAAF2* leading to male infertility as a result of PCD in a Han Chinese family. The findings may enhance the understanding of the pathogenesis of PCD and improve reproductive genetic counseling in China.

Keywords Primary ciliary dyskinesia (PCD) · male infertility · DNAAF2 mutation · spermatozoa

Introduction

Primary ciliary dyskinesia (PCD) is an autosomal recessive disease with an estimated incidence of one in 10,000–20,000 live births worldwide, although its true prevalence may be even higher [1]. PCD patients commonly suffer from chronic sinusitis, bronchiectasis, neonatal respiratory distress, male infertility, and *situs inversus*, including the randomization of

Minghan Sun and Yi Zhang contributed equally to this work.

Electronic supplementary material The online version of this article (https://doi.org/10.1007/s10815-020-01859-7) contains supplementary material, which is available to authorized users.

✉ Ke Dou
doukk@sina.cn

✉ Yongxin Ma
mayongxin@gmail.com

[1] Department of Medical Genetics and Division of Human Morbid Genomics, West China Hospital, Sichuan University, No. 37 Guo Xue Xiang, Chengdu 610041, Sichuan, China

[2] Central of Reproductive Medicine, Department of Obstetrics and Gynecology, Sichuan Academy of Medical Sciences and Sichuan Provincial People's Hospital, School of Medicine, University of Electronic Science and Technology of China, 32 Road West 2, the First Ring, Chengdu 640072, Sichuan, China

[3] The Key Laboratory for Human Disease Gene Study of Sichuan Province, Sichuan Academy of Medical Sciences and Sichuan Provincial People's Hospital, University of Electronic Science and Technology of China, Chengdu, Sichuan, China

left-right asymmetry [1, 2]. PCD was initially recognized in 1933. Since then, the laterality defects reflected in *situs inversus*, which result from the embryonic nodal cilia dysfunction known as Kartagener syndrome, have been observed in half of all PCD cases [3]. In patients with PCD, the sinuses become blocked by mucus, which may increase susceptibility to chronic respiratory infection and neonatal respiratory distress [4]. In vertebrates, multiple motile cilia and motile monocilia are distributed in different types of epithelial cells [5]. PCD is triggered by ultrastructural defects in the dysmotility of motile cilia/flagella in the respiratory epithelia, embryonic node, oviduct, and sperm [6, 7]. In some cases, dysfunctional ependymal cilia may result in reduced cerebrospinal fluid flow and hydrocephalus [1, 3]. Cilia motility depends on the dynein arms which are composed of the outer dynein arms (ODAs) and the inner dynein arms (IDAs), in the outer doublet microtubules of the axoneme. All dyneins comprise multiple subunits, which are pre-assembled in the cytoplasm before being transported to the cilia and flagella. The dynein arms are large protein complexes composed of several heavy, intermediated, and light chains [8]. Axonemal dyneins act as molecular motors capable of motivating microtubule sliding, and defects in the axonemal dyneins are commonly thought to lead to sperm immotility and male infertility [9].

Currently, approximately 40 known genes have been reported to be associated with PCD, including *DNAH5*, *DNAH11*, *DNAI1*, *DNAI2*, *DNAL1*, *TXNDC3*, *DNAAF1*, and *DNAAF2* [1, 8, 10–14]. The retardation of the ODA/IDA assembly was reported in patients carrying *DNAAF3* mutations [6]. Based on this finding, the absence of axonemal dynein axonemal assembly factors has been suggested to affect the cytoplasmic pre-assembly steps involved in the formation of axonemal dyneins. Furthermore, mutations in the *dynein axonemal assembly factor 2* (*DNAAF2*) gene have been reported to be associated with a PCD phenotype that includes male infertility [8]. The same study identified kintoun (ktu) in the medaka mutants showing organ laterality defects due to altered ciliary motility and, further, showed that ktu knockout mice exhibited a PCD-like phenotype. Additionally, the *DNAAF2* gene was reported to be involved in the pre-assembly of dynein arm complexes in some cilia.

This study investigated the clinical manifestations of PCD in a patient with male infertility from a Han Chinese family with an enriched *DNAAF2* mutation spectrum. The findings should serve to enhance the understanding of the pathogenesis of PCD.

Methods

Patients and subjects

Eight members of a Han Chinese family were recruited from the Sichuan Provincial People's Hospital to participate in this study. The clinical information of each family member is summarized in Table 1. Only the proband was diagnosed with PCD according to typical clinical findings, which include recurrent respiratory tract infections, sinusitis, bronchiectasis, and male infertility (Fig. 1a). The study was conducted in accordance with the tenets of the Declaration of Helsinki, and it was approved by the ethical committee of the Sichuan Provincial People's Hospital. Written informed consent was obtained from all family members prior to the commencement of the study. A total of 600 unrelated healthy Han Chinese control subjects were also recruited from the Sichuan Provincial People's Hospital. Subjects who had respiratory tract infections, sinusitis, bronchiectasis, and/or male infertility were excluded from the study.

Semen analysis

Fresh semen was collected from the proband, his father, and a healthy donor (control) through ejaculation after 2 to 7 days of sexual abstinence. All semen samples were tested at least three times. The samples were subjected to a staining procedure after complete liquefaction. Based on the World Health Organization's laboratory manual (2010) for the examination and processing of human semen [15], all relevant semen-related parameters with regard to the ejaculate volume, morphology, concentration, and motile spermatozoa percentage were examined. The sperm morphology was observed under an inverted phase contrast microscope (Nikon, Tokyo, Japan), and it was assessed according to the strict criteria of Kruger following the Papanicolaou staining procedure [16, 17].

For the hypo-osmotic swelling test (HOST), the semen samples were collected and then tested within 1 hour of ejaculation. The percentage of tail abnormalities (curled or swollen) was determined prior to the test. The samples were then liquefied and kept warm at 37 °C. The HOST was performed using a commercial kit (Changzhou Bei source Xin Biotechnology, Changzhou, Jiangsu, China). Briefly, 1 ml of HOST solution was heated at 37 °C for 5 min. Subsequently, 100 μl of semen was mixed with the HOST solution and incubated at 37 °C for at least 30 min. Eosin staining was performed using a commercial kit (Byxbio Biotechnology) to evaluate the viability of an aliquot of the proband's semen sample. In the eosin staining, live spermatozoa were denoted by stained white heads, and dead spermatozoa were indicated by stained red heads.

Targeted next-generation sequencing (NGS) and variant detection

Genomic DNA was collected from the participants' peripheral blood using a blood DNA extraction kit (QIAamp DNA Blood Midi Kit; Qiagen, Valencia, CA, USA). The mutation screening was performed as described in a previous study

Table 1 Family member phenotypes and genotypes

Family member	Age (year/sex)	Clinical findings	Mutation	Mutation type
I:4	87/F	-	-	-
II:1	62//F	-	c.156C>A (p.Tyr52Ter)	Heterozygous
II:2	67/M	-	c.156C>A (p.Tyr52Ter)	Heterozygous
II:3	67/F	-	c.26C>A (p.Ser9Ter)	Heterozygous
II:4	64/F	-	-	-
II:5	61/M	-	-	-
II:6	49/F	-	c.26C>A (p.Ser9Ter)	Heterozygous
III:1	40/M	Recurrent bronchitis and pneumonia, chronic sinusitis, bronchiectasis, situs inversus, infertility	c.156C>A (p.Tyr52Ter) c.26C>A (p.Ser9Ter)	Compound heterozygous

F female, *M* male; -, not available

[18]. We used a custom-designed gene panel, which was synthesized using the Agilent Sure Select Target Enrichment System, to capture the coding regions of the 210 genes, including their exons and exon-intron boundaries (1.285 Mbp in total). Three samples (III:1, II:2, and II:3) were analyzed using this targeted NGS. The bioinformatics analysis of the raw data included the following steps: (1) An image analysis was conducted using real-time analysis software (Illumina); (2) base calling was performed using CASAVA software v1.8.2 (Illumina); (3) the duplicate and low base quality reads were filtered out using the Genome Analysis Tool Kit (GATK); (4) the clean paired-end reads were aligned with the human

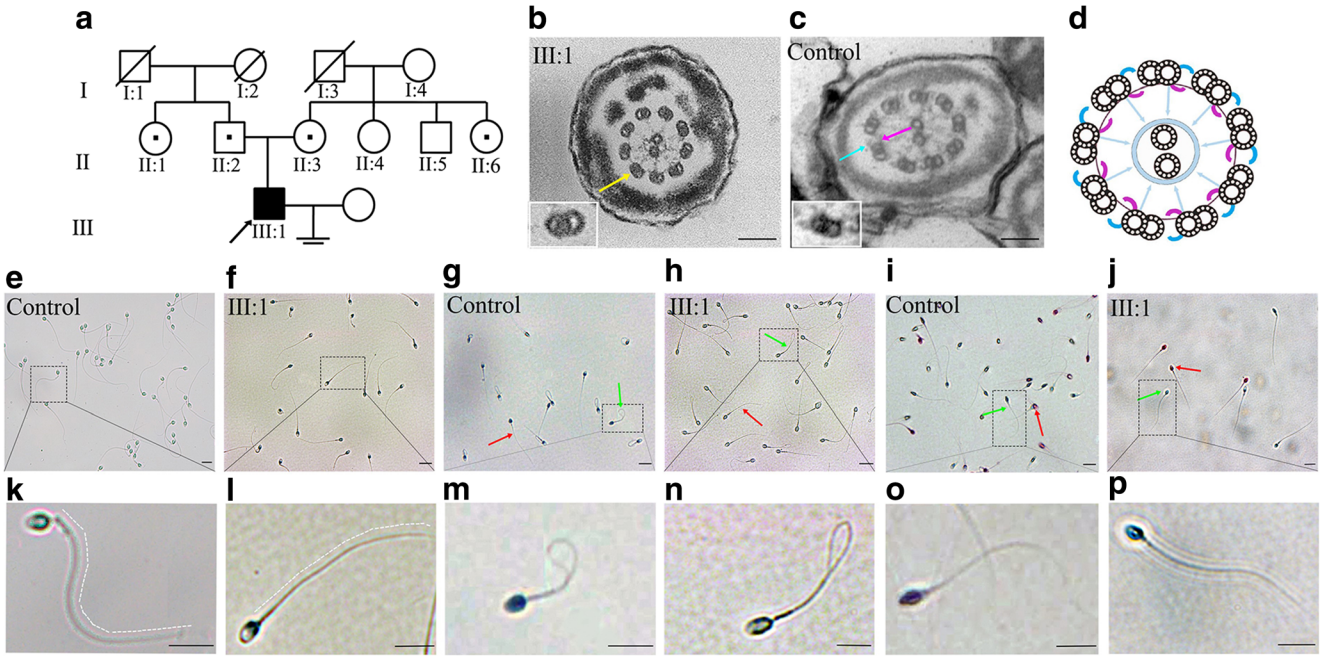

Fig. 1 Pedigree of the family with PCD and the clinical features of the proband from this family. **a** There is one patient (the proband) in the family with PCD. The solid symbols indicate the affected individuals, the open symbols indicate the unaffected individuals, the dots in the circles and boxes show the subject who is a carrier of the identified mutations, and the arrow indicates the proband. **b** The transmission electron micrograph (TEM) of the sperm flagella cross-section from the proband (III:1) shows the complete loss of the outer and inner dynein arm defects (yellow arrowhead). Scale bar, 200 nm. **c** The ultrastructure analysis of the axonemal cross-section of the sperm flagella obtained from a healthy donor (control) by TEM, which shows the characteristic "9 + 2" arrangement of the microtubules, including the ODAs (blue arrowhead) and IDAs (purple arrowhead). **d** A schematic diagram of the sperm flagella cross-section. **e–f** The microphotograph of the spermatozoa shows the progressive and non-progressive motility of the healthy donor (**e**) and the proband (**f**). Scale bar, 10 μm. **g–j** The microphotograph of the spermatozoa following with the hypo-osmotic swelling test (HOST, **g** and **h**) and eosin staining (**i** and **j**) shows viable immotile sperm in the spermatozoa from the proband (**g** and **i**) and the healthy donor (**h** and **j**). The live sperm tail was swelling and curling (**g** and **h**, green arrowhead), the spermatozoa in white are alive (**i** and **j**, green arrowhead), while the one stained in red is dead (**i** and **j**, red arrowhead). The boxed regions (**k–p**) are magnified below. Scale bar, 10 μm

reference genome build hg19 using BWA software (Pittsburgh Supercomputing Center, Pittsburgh, PA, USA); and (5) the insertion-deletion mutations (indels) and single-nucleotide polymorphisms (SNPs) were identified using the GATK and then annotated using ANNOVAR software. The sequencing depth was more than × 5 (range of × 5–× 185; average of × 136), and the mean coverage was 98.74%. The detected variants were annotated and filtered based on both public and in-house databases. The validation and parental origin analyses of these variations were performed by conventional Sanger sequencing. The *DNAAF2* (NM_001083908.1, https://www.ncbi.nlm.nih.gov/nuccore/NM_001083908.1) mutations identified by the targeted NGS were confirmed in all the family members and in the 600 normal controls using direct sequencing. The primers flanking the mutations were designed based on the genomic sequences listed in the Human Genome Database and then synthesized by Invitrogen Life Technologies (Shanghai, China): *DNAAF2*-F, AGAAACTCTGAGGA GGATCC, and *DNAAF2*-R, TTCAGGGTCTTGGC ATTCCT. The coding region of *DNAAF2* was analyzed in both directions using an automated genetic analysis system (ABI 3130 Genetic Analyzer, Applied Biosystems, Foster City CA, USA). The multiple sequence alignment of the human DNAAF2 protein was analyzed, together with the alignments of other DNAAF2 proteins, across the orthologs to examine the conservation of the residues.

Western blot analysis

The spermatozoa samples obtained from the proband, his father, and a healthy donor (control) were placed on ice for 30 min in radioimmunoprecipitation (RIPA) buffer containing 50 mM Tris-HCl (Sigma), 150 mM sodium chloride, 1% Nonidet P-40 (Sigma), 0.25% sodium deoxycholate (Sigma), a protease inhibitor cocktail (Roche), and 1 mM phenylmethylsulfonylfluoride (PMSF; Sigma). The sperm lysates were run in a 10% SDS-PAGE gel and then transferred to a nitrocellulose membrane (Millipore). The membranes were blocked for 1 h at room temperature with 5% skim milk in Tris-buffered saline containing 0.05% Tween 20. This was followed by incubation overnight at 4 °C with horseradish peroxidase (HRP)-conjugated antibodies raised against DNAAF2 (Sigma, HPA004113) and β-actin (Sigma, A5441). The immunogen sequence of the DNAAF2 antibody is from the 518th to the 621th amino acid (GEPLCPPLLCNQDKETLTLLIQVPRIQPQSLQGDLNPL-WYKLRFSAQDLVYSFFLQFAPENKLSTTEPVISISSNNA-VIELAKSPESHGHWREWYYGVNNDSLE). The signals were visualized using an enhanced chemiluminescence kit (Thermo Scientific), while an Image Quant LAS4000 Mini Luminescent Image Analyzer was used for the image acquisition (GE Healthcare).

Immunofluorescence staining

The spermatozoa samples obtained from the proband, his father, and a healthy donor (control) were spread onto microscope slides and allowed to air-dry. Then, they were fixed with 4% paraformaldehyde, 0.2% Triton X-100, and 1% skim milk. The samples were incubated with rabbit polyclonal anti-DNAAF2 (Sigma, HPA004113), rabbit polyclonal anti-DNAH9 (Thermo Fisher, PA5-57958), rabbit polyclonal anti-DNAH5 (Thermo Fisher, PA5-45744), rabbit polyclonal anti-DNALI1 (Sigma, HPA028305), and mouse monoclonal anti-acetylated (K40) α-tubulin (Abcam, ab24610). They were incubated with secondary antibodies including FITC-conjugated goat anti-rabbit IgG polyclonal antibody (Jackson, 111-095-003) and FITC-conjugated goat anti-mouse IgG antibody (Jackson, 115-095-003). After staining with 4',6-diamidino-2-phenylindole (DAPI, Sigma, D9542), the samples were washed and then analyzed immediately under a confocal microscope (Olympus, Tokyo, Japan).

Transmission electron microscopy (TEM)

The aliquot of the proband's sperm was fixed with 2.5% glutaraldehyde (Sigma) in 0.1 M sodium cacodylate buffer (Sigma) and 1% osmium tetroxide (Sigma) at 4 °C. Following dehydration, the samples were embedded in epoxy resin (Sigma). Thin sections stained with Reynold's lead citrate were imaged using a Philips CM10 EM. The images were captured using a charge-coupled device camera (Olympus, Tokyo, Japan).

Results

Clinical features

This study consisted of eight members (three generations) from a non-consanguineous family with PCD in Sichuan Province, China (Fig. 1a). The proband (III:1) exhibited typical PCD-related clinical symptoms, including chronic otitis media, and recurrent pneumonia since birth (Table 1). The computed tomography examination of the proband showed chronic ethmoid and maxillary sinusitis, ring-shaped or ductal opacities throughout both lungs, bilateral lung bronchiectasis, and *situs inversus* totalis in the heart, liver, and colon (Supplementary Fig. 1). The other seven family members did not exhibit these clinical findings. To investigate the ultrastructure of the spermatozoa flagella, TEM scanning of the proband's sperm flagella was performed. The proband's sperm flagella showed complete axonemal defects in both the ODAs and IDAs (Fig. 1b), compared with the normal structure of sperm [10] (Fig. 1c and 1d). The proband's semen was normal in terms of ejaculate volume, viscosity, liquefaction, pH, and sperm concentration. However, there were multiple

Table 2 Semen analysis of the spermatozoa from the proband, his father, and a control

Parameters	Proband (mean/range)	Proband's father*	Control (mean/range)
Volume (ml)	2.8 (2.5–3.2)	1.6	3.1 (2.7–3.7)
Potential of hydrogen (PH)	7.4 (7.3–7.5)	7.3	7.2 (7.1–7.5)
Concentration (10^6/ml)	27.5 (23.0–31.7)	17.2	32.4 (27.2–34.5)
Progressive motility (PR) (%)	0	12.6	42.0 (39.2–45.8)
Non-progressive motility (NP) (%)	0	1.5	8.6 (7.2–9.6)
Immotility (IM) (%)	100	85.9	49.4 (44.6–53.6)
Viability (HOST) (%)	46.9 (46.5–47.8)	-	48.0 (44.3–52.5)
Viability (eosin staining) (%)	53.2 (51.5–53.4)	-	54.8 (52.3–56.8)
Live spermatozoa (HOST) (10^6/ml)	12.9	-	15.6
Live spermatozoa (eosin staining) (10^6/ml)	14.6	-	17.8
Dead spermatozoa (HOST)	14.6	-	16.8
Dead spermatozoa (eosin staining) (10^6/ml)	12.9	-	14.6
Abnormal spermatozoa (%)	97.0 (96.2–98.3)	96.3	93.0 (92.7–94.5)

*As the proband's father (II:2) is 67 years old, he could only provide additional semen specimens just once due to health concerns. -, Not available

morphological defects in the heads (thin head, and pyriform heads) and tails of the proband's spermatozoa, and approximately 97% of the spermatozoa showed morphological anomalies (Table 2 and Supplementary Fig. 2). Compared with the motility of the healthy donor's spermatozoa (Fig. 1e and k), the progressive and non-progressive motility of the proband's spermatozoa were both 0 (Table 2) and indicated the complete immotility of the spermatozoa (Fig. 1f and l). The high-speed video microscopy demonstrated the complete immotility of the proband's sperm flagella compared with that of the healthy control (Supplementary Movies 1–2). The HOST (Fig. 1g and h) and eosin staining (Fig. 1i and j) showed that the proband had the same viability in terms of the immotile spermatozoa (the scores were 46.92% and 53.21%, respectively) as that seen in a healthy donor (the scores were 48.0% and 58.8%, respectively; Table 2).

Targeted NGS and mutation validation

To ensure the complete sequencing coverage of all the coding regions in *DNAAF2*, the quality and reliability of the NGS data were evaluated based on the percentage of readable bases and the coverage depth within the targeted region. In the *DNAAF2* gene, the coverage depth was up to × 200, with 100% of the bases being readable in the coding regions. This suggests a high capacity for variant identification in most of the exons. Additionally, the mean depth was close to the median depth in each exon, thereby indicating good randomicity. On average, 212 variations within the 210 genes were found in the three tested subjects (III:1, II:2, and II:3). For the analysis of the autosomal recessive model, we first focused on the functional SNPs/indels in the homozygous or compound heterozygous variants, including the frameshift coding region insertions or deletions, splice acceptor and donor-site mutations, and non-synonymous variants, which were more likely to be pathogenic. Then, we excluded these common variants with a high frequency using the dbSNP138, YH Database, HapMap Project, 1000 Genome Project, Exome Aggregation Consortium, and our in-house database. In addition, we further compared these filtered variants with previously reported PCD-related genes. Finally, the filtered data were narrowed down to two novel compound heterozygous mutations, c.C156A [p.Y52X] and c.C26A [p.S9X], in the *DNAAF2* gene. The two variants were validated using Sanger sequencing performed on the other family members and on the 600 normal controls. We confirmed that the two novel compound heterozygous mutations in the *DNAAF2* gene were completely co-segregated within the PCD family (Figs. 1 and 2). The two nonsense mutations led to a truncated protein at nucleotide 26 and 156 of exon 1, respectively (Fig. 2a). Both mutations were present in the proband (III:1), and each of his parents was an unaffected carrier of one of the mutations. The proband's father carried the mutation c.156C>A, while the proband's mother carried the mutation c.26C>A (Table 1). The other unaffected family members carried either none or just one of the two mutations (Table 1). The two nonsense heterozygous mutations were not detected in any of the 600 ethnically matched normal controls. The orthologous protein sequence alignment of DNAAF2 across the orthologs revealed that the two mutations occurred at highly conserved positions (Fig. 2c).

Mutations in *DNAAF2* led to the dysfunction of the DNAAF2 protein in spermatozoa

To further investigate the molecular mechanisms responsible for the dysfunction of human spermatozoa, we analyzed the

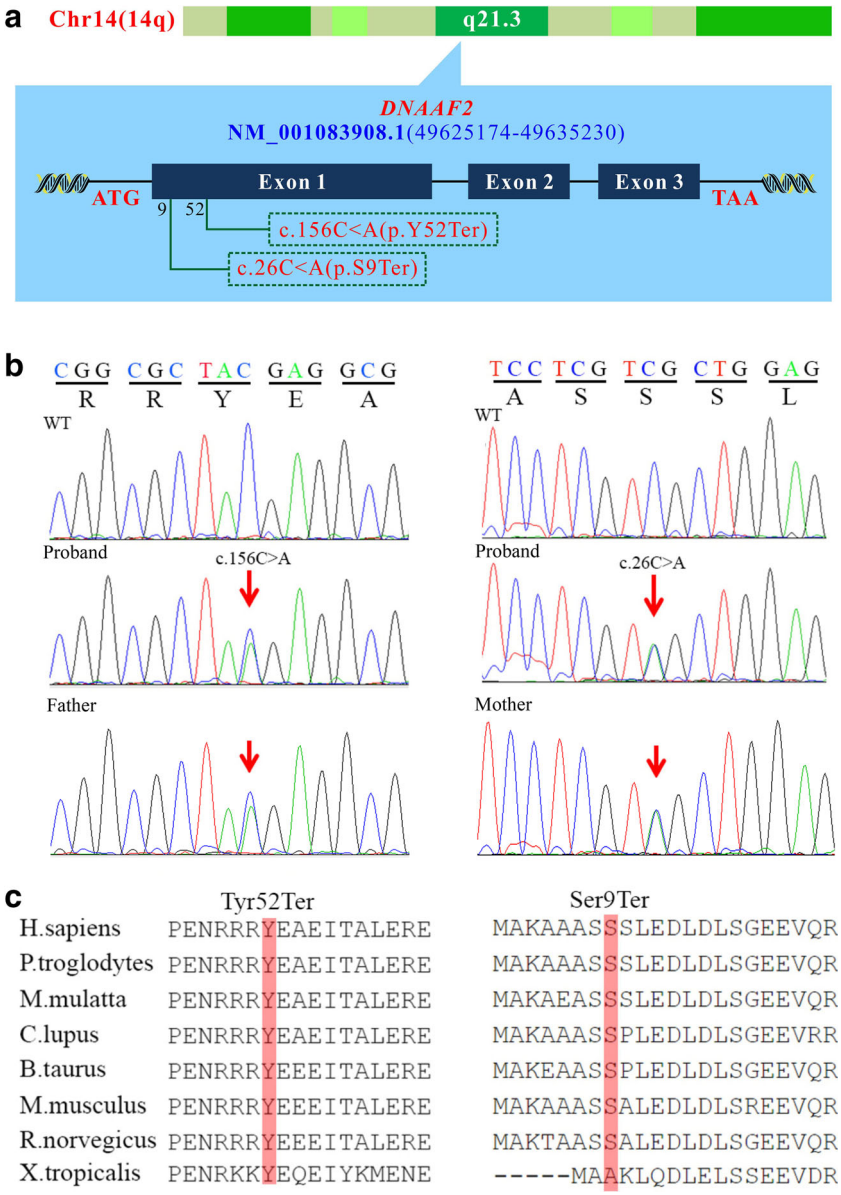

Fig. 2 Representative chromatogram of the *DNAAF2* sequence. **a** Mutations in the *DNAAF2* gene were identified in the family with PCD. The boxed mutations in red were newly found in this study. **b** Direct sequencing identified two novel compound heterozygous mutations (left, c.156C>A (p.Tyr52Ter); (right, c.26C>A (p.Ser9Ter)) in *DNAAF2* (NM_001083908.1). **c** Orthologous protein sequence alignment of *DNAAF2* from different species. The red-shaded box shows that the two novel mutations occurred at highly conserved positions in these species

presence of DNAAF2 in spermatozoa samples obtained from the proband (III:1), his father, and a healthy donor (control). The immunofluorescence staining analysis revealed that DNAAF2 was absent from the proband's spermatozoa. It was weak in the spermatozoa obtained from his father but was correctly localized in the sperm cytoplasm but not in the flagellum in the spermatozoa obtained from the healthy control (Fig. 3a–c). These findings are consistent with those of previous studies [8, 19]. Moreover, according to the Western blot analysis, there was almost no DNAAF2 expression in the spermatozoa obtained from the proband, whereas the DNAAF2 expression dramatically decreased in the spermatozoa from the proband's father compared with the healthy control (Fig. 3d–e). To characterize the ultrastructural defects observed by TEM at the molecular level, we performed immunostaining using antibodies targeting various axonemal proteins. The double immunostaining results showed defects in DNAH9 and DNALI1 and only some residual staining in DNAH5 in the proximal ciliary axoneme of the respiratory cells from the proband compared with the healthy control (Fig. 4). DNAH9 and DNALI1 were not detectable, and there was only a weak staining of DNAH5 in the sperm tails of the proband compared with the healthy control (Fig. 5).

Discussion

The cilia and flagella are highly conserved organelles that control both cell motility and sense extracellular signals. Motility defects in the cilia and flagella often cause PCD [8]. This complex disease phenotype, which results from the abnormal functioning of embryonic respiratory nodal cilia and

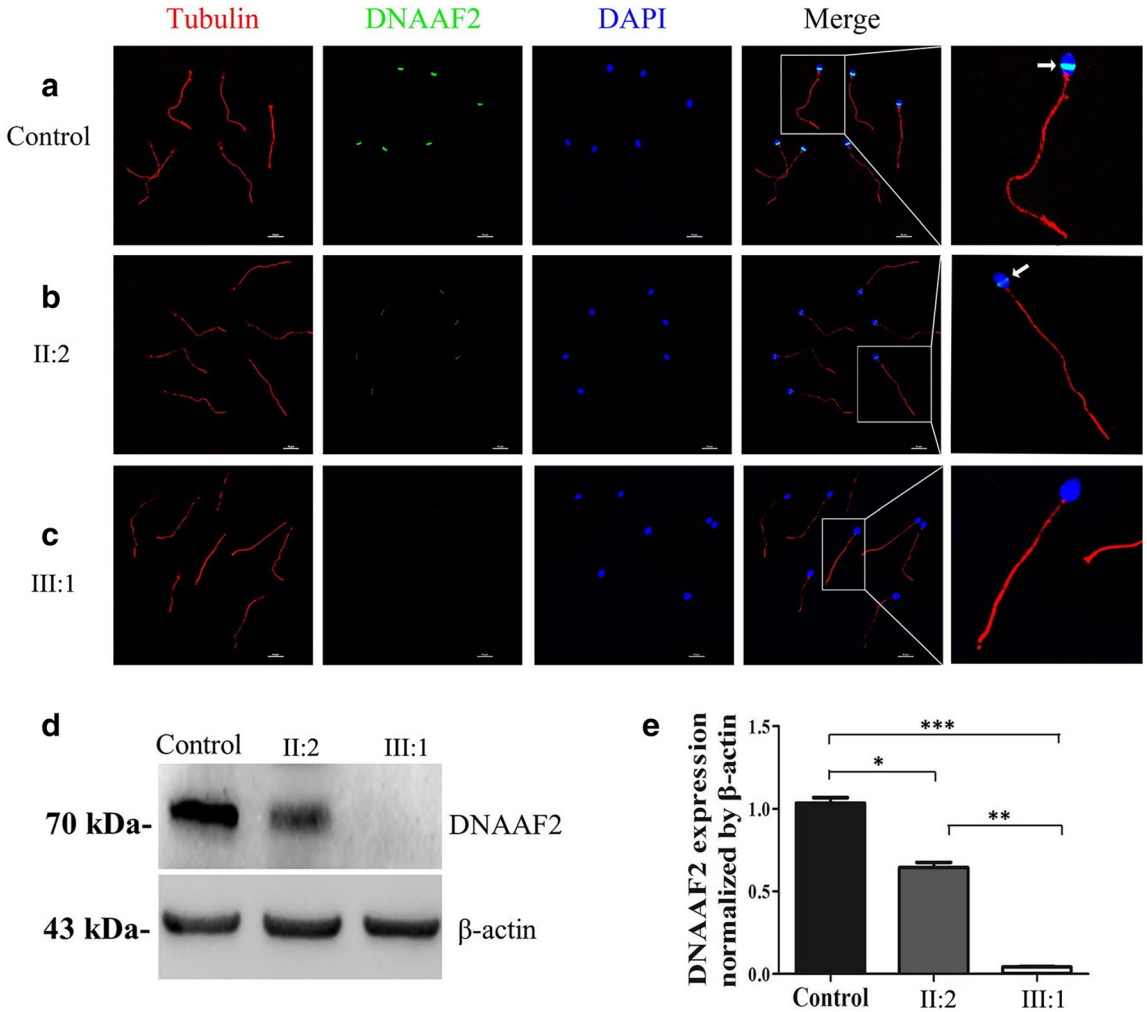

Fig. 3 DNAAF2 expression in the spermatozoa from the proband, his father, and a healthy control. **a–c** The immunofluorescence images show that tubulin (red) was present in all the spermatozoa tails. The expression of DNAAF2 (green) was absent from the proband's spermatozoa and weak in his father's spermatozoa (II:2), whereas it was correctly localized in the cytoplasm of the spermatozoa from the healthy control. The nuclei were stained with 4',6-diamidino-2-phenylindole (DAPI). The boxed regions are magnified to the right. Scale bar, 10 μm. **d–e** Western blot showed no DNAAF2 in the proband's spermatozoa. The expression of DNAAF2 protein was significantly decreased in his father's spermatozoa (II:2) and dramatically decreased in the spermatozoa of the proband compared with the healthy control. The expression of the housekeeping protein β-actin is shown as a reference. The asterisk indicates a $p < 0.05$ according to Student's independent t test. All the experiments were conducted in triplicate

sperm flagella, is inherited in a Mendelian manner [8, 20]. After *DNAI1* was first identified as a pathogenic gene in PCD patients with immotile respiratory cilia in 1999 [11], other mutations have been discovered in PCD patients from various populations worldwide. In the present study, we reported two novel compound heterozygous mutations, c.C156A [p.Y52X] and c.C26A [p.S9X], in the *DNAAF2* gene that led to male infertility in a Han Chinese family with PCD. These findings may enhance the understanding of the molecular pathogenesis of *DNAAF2*-associated PCD.

The human *DNAAF2* gene, which is located at chromosome 14q21.3, encodes a highly conserved DNAAF2 protein. This protein is distributed in ciliated cell types, and it interacts with several proteins that localize to the cilia. As a major member of the DNAAF protein family, DNAAF2 is involved in the pre-assembly of the dynein arm complexes in the cytoplasm prior to their transportation to the ciliary compartment [8]. This study reported that *DNAAF2* mutations in human caused combined ODA and IDA defects that lead to PCD [8]. A previous study also identified mutations in the human *DNAAF3* gene in patients with *situs inversus* and defects in the ODA and IDA assembly [6].

In this study, the genetic analysis of the *DNAAF2* gene helped to confirm the diagnosis of the proband in the pedigree. The affected individual (III:1) carried two novel compound heterozygous mutations c.C156A [p.Y52X] and c.C26A [p.S9X] in exon 1 of the *DNAAF2* gene (Fig. 2). Two homozygous mutations, (c.C23A [pS8X] and c.1214-1215insACGATACCTGCGTGGC [p.G406Rfs89X]), in the *DNAAF2* gene were identified in two PCD patients in a

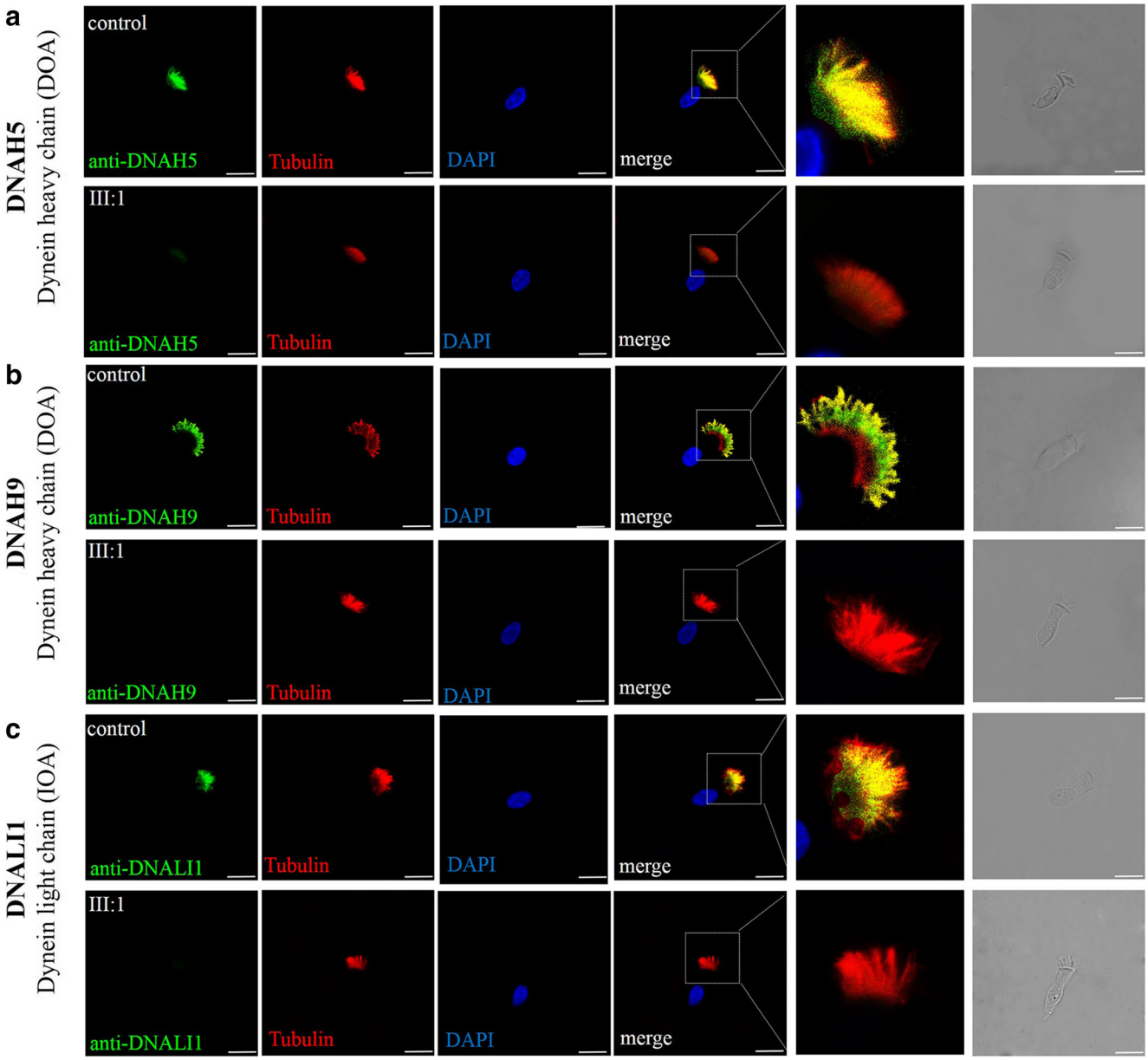

Fig. 4 Immunofluorescence microscopy of respiratory epithelial cells from a healthy control and the proband using specific antibodies directed against the outer dynein arms (ODAs) with DNAH5 and DNAH9 and against the inner dynein arms (IDAs) with DNALI1. **a** There is only some residual staining for DNAH5 in the proximal ciliary axoneme in the respiratory cells from the proband compared with the healthy control. **b** Double immunostaining with the antibody against DNAH9 and tubulin showed the co-localization of the control ciliated cells in the distal part of the ciliary axoneme as well as complete absence of DNAH9 in the respiratory cells of the proband. **c** Double immunostaining with the antibody against DNALI1 and tubulin showed the co-localization of control ciliated cells in the distal part of the ciliary axoneme and the complete absence of DNALI1 in the respiratory cells of the proband. Tubulin was stained as the control for ciliary axonemes. The nuclei were stained with 4',6-diamidino-2-phenylindole (DAPI). Scale bar, 10 μm

previous study [8]. This is the first study to report two compound heterozygous mutations of *DNAAF2* in a patient with PCD. In 2018, another two heterozygous mutations, c.T1901C [p.F634S] and c.C998T [p.A333V], in the DNAAF2 gene were identified in a Dutch PCD population [21]. In this pedigree, the affected individual (III:1) harbored both mutations in the *DNAAF2* gene, and no other alteration was detected in the coding region of the *DNAAF2* gene in the proband with male infertility. The proband was further diagnosed with PCD when he suffered from male infertility and went to a hospital for evaluation. The other family members did not exhibit the same clinical findings. The mutation analysis revealed that the proband's father (II:2) and uncle (II:1) carried the c.C156A [p.Y52X] mutation, while his mother (II:3) and aunt (II:6) carried the c.C26A [p.S9X] mutation (Table 1). The two mutations in *DNAAF2* were not detected

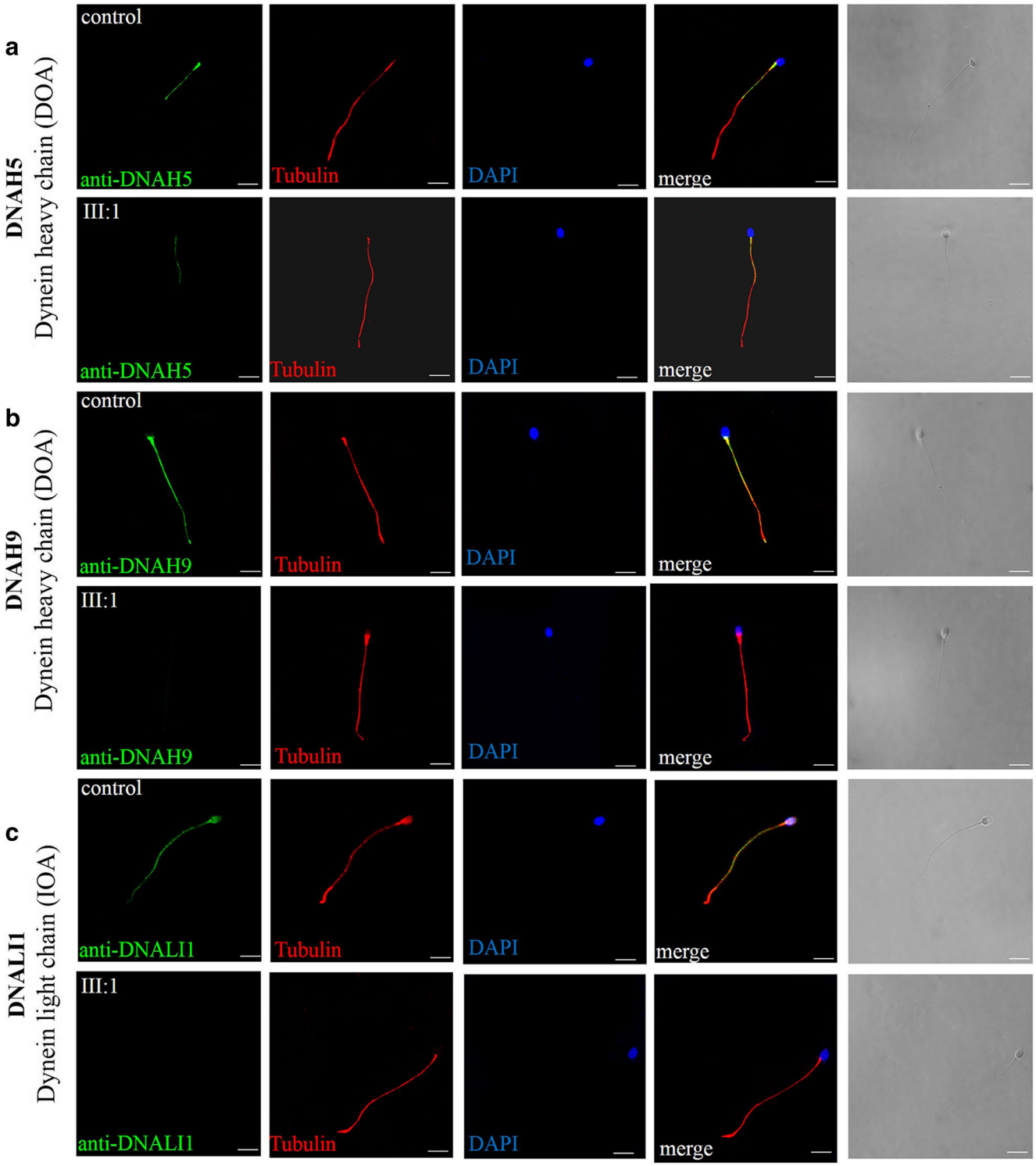

Fig. 5 Immunofluorescence microscopy of the human spermatozoa from a healthy control and the proband using specific antibodies directed against the outer dynein arms (ODAs) with DNAH5 and DNAH9 and against inner dynein arms (IDAs) with DNALI1. **a–c** DNAH9 and DNALI1 were not detectable, and weak staining of DNAH5 was found in the sperm tails of the proband. By contrast, DNAH5 was localized exclusively to the proximal part of the sperm tail of the control, and DNAH9 and DNALI1 were localized to the entire sperm flagellum in the control sperm axoneme. Tubulin was stained as a control for the ciliary axonemes. The nuclei were stained with 4',6-diamidino-2-phenylindole (DAPI). Scale bar, 10 μm

in any of the 600 healthy controls nor in the public databases searched (including ExAC and Genome AD), thus suggesting that autosomal recessive inheritance occurred in the family. Therefore, it is reasonable to hypothesize that the two novel

mutations of the *DNAAF2* gene identified in the present study are responsible for the PCD pathogenesis in this pedigree.

Several PCD genes including *DNAAF2*, *DNAH5*, *DNAH11*, *DNAI1*, *DNAI2*, and *DNAL1*, *DNAAF1*, and *DNAAF3* are reported to affect the assembly of both ODA and IDA complexes, and a central pair is surrounded by nine peripheral doublets of microtubules (Fig. 6a). As indicated by the TEM scanning in this study, the ultrastructure of the ODAs and IDAs of the proband's sperm flagella appeared abnormal compared with the normal ultrastructural arrangement of the flagella (i.e., a typical "9 + 2"pattern, with two central and nine pairs of peripheral microtubules) (Fig. 6a). The spermatozoa of the proband who carried the *DNAAF2* mutations were completely immobile, although they exhibited relatively high viability. These results are consistent with those obtained by Omran et al. [8] who showed that male mutant fish exhibited impaired sperm motility, which led to reduced fertility. The mutations in the genes that encode the dynein subunits, or the components required for the assembly, transport, or docking of axonemal dyneins, result in a wide range of developmental defects and diseases. Mass spectrometric analyses of the DNAAF2 immunoprecipitates obtained from murine testis extracts identified heat-shock protein 70 (Hsp70) [8], thereby suggesting that this protein functions as a co-chaperone with Hsp70 to facilitate the correct assembly of the dynein complexes in the cytoplasm before they are transported to the cilia and flagella as shown in Fig. 6. It is possible that the *DNAAF2* mutations were responsible for the complete immotility of the spermatozoa obtained from the proband in the present study. The serine/tyrosine codons in DNAAF2 were replaced by the termination codon in exon 1, which resulted in a truncated protein of DNAAF2. The proband carried both the *DNAAF2* nonsense mutations, which could lead to a dysfunctional protein, and ultimately he

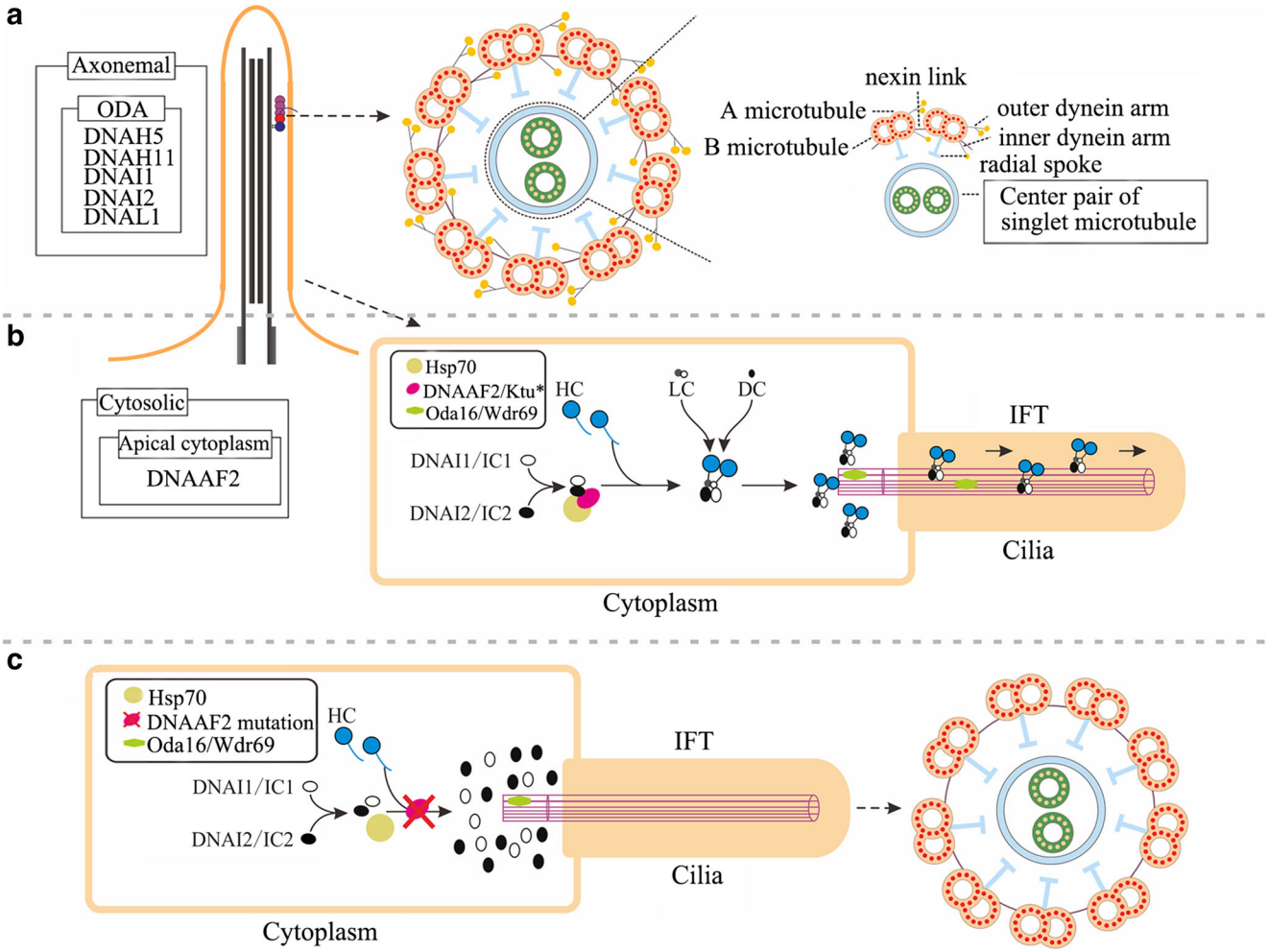

Fig. 6 Schematic diagram of the hypothesized role of *DNAAF2* in the dynein arm assembly for PCD development. **a** The PCD genes, including *DNAAF2*, *DNAH5*, *DNAH11*, *DNAI1*, *DNAI2*, and *DNAL1*, are located in the axoneme, and a central pair is surrounded by nine peripheral doublets of microtubules. **b** DNAAF2 is involved in the assembly of the dynein arm complexes, which are responsible for the generation of the force required for movement. **c** The *DNAAF2* mutation causes the ODAs and IDAs to be absent from the axoneme before they are transported to their intended functional sites. IC2, intermediate chain 2; DNAI2, dynein axonemal intermediate 2; Hsp70, heat-shock protein 70; IC1, intermediate chain 1; HC, heavy chain; LC, light chain; DC, docking complex; IFT, intraflagellar transport

suffered from impaired fertility. Compared with the proband, his father carried one of the nonsense mutations and still had an unaffected phenotype (including chronic ethmoid and maxillary sinusitis, ring-shaped or ductal opacities throughout the lungs, bilateral lung bronchiectasis, and *situs inversus* totalis in the heart, liver, and colon). These clinical features were consistent with our Western blot analysis, which showed no positive signaling of DNAAF2 in the sperm lysis from the proband and a low positive signaling in the sperm lysis from the proband's father. Therefore, the mutations in the *DNAAF2* gene may be loss-of-function mutations and closely associated with the pre-assembly of dynein arm complexes, which provide energy for the cilia. As expected, our data showed defects in the ODAs (DNAH5 and DNAH9) and IDAs (DNALI1) in the respiratory cilia and spermatozoa obtained from the proband (Figs. 4 and 5). This specific defect, which results from the dysfunctionalDNAAF2 protein or the lack of DNNAF2 protein synergy in the spermatozoa, may cause an abnormal ODA and IDA assembly and the complete immotility of the sperm cells, thereby demonstrating the essential role played by DNAAF2 in axonemal assembly (Fig. 6b and c). As shown in Fig. 6b, it was previously proposed that the dynein arms are pre-assembled as three complexes, an intermediate chain-heavy chain (IC–HC) complex, a light chain (LC) complex, and a docking complex (DC) [19]. If IC could not combine with HC to form IC-HC complex, the formation of ciliary complex may be blocked; thus, it could not be transported to the cilia through intraflagellar transport (IFT) to complete axonemal assembly (Fig. 6c). However, the exact pathological mechanisms underlying the effect of these two novel mutations of the *DNAAF2* gene on the development of the PCD phenotype remain unclear. In fact, there were two populations of spermatozoa from his father, including one with a mutant allele and another with a wild-type (WT) allele. If we could identify the two populations of his father's spermatozoa, including the one with normal expression of DNAAF2 from the WT allele and the other one with no or reduced expression of DNAAF2 from the T52X allele, it would be helpful in understanding the spermatogenesis of patient with PCD. Therefore, it is necessary for us to recruit more male carriers with *DNAAF2* mutations, to provide more evidence, and to further validate our data on Chinese PCD subjects in the future.

Taken together with the clinical characteristics of the proband, the findings of this study suggest that the c.C156A [p.Y52X] and c.C26A [p.S9X] mutations of the *DNAAF2* gene are pertinent to male infertility in the investigated family with PCD. This study enriches our knowledge of the *DNAAF2* mutation spectrum in the PCD, and the findings may contribute to enhancing the understanding of the pathogenesis of PCD and improving reproductive genetic counseling in China.

References

1. Mirra V, Werner C, Santamaria F. Primary ciliary dyskinesia: an update on clinical aspects, genetics, diagnosis, and future treatment strategies. Front Pediatr. 2017;5:135.
2. Lee L. Mechanisms of mammalian ciliary motility: insights from primary ciliary dyskinesia genetics. Gene. 2011;473(2):57–66. https://doi.org/10.1016/j.gene.2010.11.006.
3. Sha YW, Ding L, Li P. Management of primary ciliary dyskinesia/Kartagener's syndrome in infertile male patients and current progress in defining the underlying genetic mechanism. Asian J Androl. 2014;16(1):101–6.
4. Bisgrove BW, Yost HJ. The roles of cilia in developmental disorders and disease. Development. 2006;133(21):4131–43. https://doi.org/10.1242/dev.02595.
5. El Zein L, Omran H, Bouvagnet P. Lateralization defects and ciliary dyskinesia: lessons from algae. Trends Genet. 2003;19(3):162–7. https://doi.org/10.1016/s0168-9525(03)00026-x.
6. Mitchison HM, Schmidts M, Loges NT, Freshour J, Dritsoula A, Hirst RA, et al. Mutations in axonemal dynein assembly factor DNAAF3 cause primary ciliary dyskinesia. Nat Genet. 2012;44(4):381–9. https://doi.org/10.1038/ng.1106 s1-2.
7. Afzelius BA. Cilia-related diseases. J Pathol. 2004;204(4):470–7. https://doi.org/10.1002/path.1652.
8. Omran H, Kobayashi D, Olbrich H, Tsukahara T, Loges NT, Hagiwara H, et al. Ktu/PF13 is required for cytoplasmic pre-assembly of axonemal dyneins. Nature. 2008;456(7222):611–6. https://doi.org/10.1038/nature07471.
9. Ibanez-Tallon I, Heintz N, Omran H. To beat or not to beat: roles of cilia in development and disease. Hum Mol Genet. 2003;12 Spec(No 1):R27-35.
10. Bartoloni L, Blouin JL, Pan Y, Gehrig C, Maiti AK, Scamuffa N, et al. Mutations in the DNAH11 (axonemal heavy chain dynein type 11) gene cause one form of situs inversus totalis and most likely primary ciliary dyskinesia. Proc Natl Acad Sci U S A. 2002;99(16):10282–6. https://doi.org/10.1073/pnas.152337699.
11. Pennarun G, Escudier E, Chapelin C, Bridoux AM, Cacheux V, Roger G, et al. Loss-of-function mutations in a human gene related to Chlamydomonas reinhardtii dynein IC78 result in primary ciliary dyskinesia. Am J Hum Genet. 1999;65(6):1508–19. https://doi.org/10.1086/302683.
12. Mazor M, Alkrinawi S, Chalifa-Caspi V, Manor E, Sheffield VC, Aviram M, et al. Primary ciliary dyskinesia caused by homozygous mutation in DNAL1, encoding dynein light chain 1. Am J Hum Genet. 2011;88(5):599–607. https://doi.org/10.1016/j.ajhg.2011.03.018.
13. Duriez B, Duquesnoy P, Escudier E, Bridoux AM, Escalier D, Rayet I, et al. A common variant in combination with a nonsense mutation in a member of the thioredoxin family causes primary ciliary dyskinesia. Proc Natl Acad Sci U S A. 2007;104(9):3336–41. https://doi.org/10.1073/pnas.0611405104.
14. Duquesnoy P, Escudier E, Vincensini L, Freshour J, Bridoux AM, Coste A, et al. Loss-of-function mutations in the human ortholog of Chlamydomonas reinhardtii ODA7 disrupt dynein arm assembly and cause primary ciliary dyskinesia. Am J Hum Genet. 2009;85(6):890–6. https://doi.org/10.1016/j.ajhg.2009.11.008.
15. WHO. WHO Laboratory Manual for the Examination and Processing of Human Semen. Fifth ed; 2010.

16. Kruger TF, DuToit TC, Franken DR, Acosta AA, Oehninger SC, Menkveld R, et al. A new computerized method of reading sperm morphology (strict criteria) is as efficient as technician reading. Fertil Steril. 1993;59(1):202–9.
17. Kruger TF, Ackerman SB, Simmons KF, Swanson RJ, Brugo SS, Acosta AA. A quick, reliable staining technique for human sperm morphology. Arch Androl. 1987;18(3): 275–7.
18. Pang M, Liu Y, Hou X, Yang J, He X, Hou N, et al. A novel APC mutation identified in a large Chinese family with familial adenomatous polyposis and a brief literature review. Mol Med Rep. 2018;18(2):1423–32.
19. Fowkes ME, Mitchell DR. The role of preassembled cytoplasmic complexes in assembly of flagellar dynein subunits. Mol Biol Cell. 1998;9(9):2337–47.
20. Badano JL, Mitsuma N, Beales PL, Katsanis N. The ciliopathies: an emerging class of human genetic disorders. Annu Rev Genomics Hum Genet. 2006;7:125–48.
21. Paff T, Kooi IE, Moutaouakil Y, Riesebos E, Sistermans EA, Daniels H, et al. Diagnostic yield of a targeted gene panel in primary ciliary dyskinesia patients. Hum Mutat. 2018;39(5):653–65.